Transmittance Multispectral Imaging for Adulteration Assessment of Coconut Oil

Conference Paper · September 2021

DOI: 10.1109/ICIIS53135.2021.9660746

Neranjan Senarath
University of Peradeniya

Dhananjaya Jayasundara
University of Peradeniya

Lakshitha Sanchuka
University of Peradeniya

Don Yasiru Lakshan Ranasinghe
University of Peradeniya

Transmittance Multispectral Imaging for Adulteration Assessment of Coconut Oil

Neranjan Senarath
Department of Electrical and Electronic Engineering University of Peradeniya
Peradeniya 20400,Sri Lanka
e15332@eng.pdn.ac.lk

Dhananjaya Jayasundara
Department of Electrical and Electronic Engineering University of Peradeniya
Peradeniya 20400,Sri Lanka
e15157@eng.pdn.ac.lk

Lakshitha Ramanayake
Department of Electrical and Electronic Engineering University of Peradeniya
Peradeniya 20400,Sri Lanka
lakshitharamanayake@eng.pdn.ac.lk

D.Y.L. Ranasinghe
Department of Electrical and Electronic Engineering University of Peradeniya
Peradeniya 20400,Sri Lanka
e14273@eng.pdn.ac.lk

Sanjaya Lakmal
Department of Electrical and Electronic Engineering University of Peradeniya
Peradeniya 20400,Sri Lanka
sanjaya.h@eng.pdn.ac.lk

H.M.H.K. Weerasooriya
Department of Electrical and Electronic Engineering University of Peradeniya
Peradeniya 20400,Sri Lanka
kavingaweerasooriya@eng.pdn.ac.lk

Parakrama Ekanayake
Department of Electrical and Electronic Engineering University of Peradeniya
Peradeniya 20400,Sri Lanka
mpb.ekanayake@ee.pdn.ac.lk

Roshan Godaliyadda
Department of Electrical and Electronic Engineering University of Peradeniya
Peradeniya 20400,Sri Lanka
roshangodd@ee.pdn.ac.lk

Vijitha Herath
Department of Electrical and Electronic Engineering University of Peradeniya
Peradeniya 20400,Sri Lanka
vijitha@eng.pdn.ac.lk

W.M.T. Madhujith
Department of Food Science and Technology University of Peradeniya 20400 Sri Lanka
tmadhujith@agri.pdn.ac.lk

***Abstract*— Coconut oil extracted from the kernel of coconut is a commonly used edible oil. This which have many health benefits and nutritional value has been one of the main components in food industry. Adulterating different edible oils with coconut oil has reduced its' quality causing major health issues. In this paper an algorithm is proposed to identify the adulteration level of coconut oil adulterated using reheated/ reused coconut oil. For this, transmittance multispectral images captured using an inhouse built economical multispectral imaging device is used. A Principal Component Analysis based Bhattacharyya distance model is developed with a 0.9747 coefficient of determination.**

***Keywords*— Coconut Oil, Multi-Spectral Image (MSI), Reheated/Reused, Principal Component Analysis (PCA), Bhattacharyya Distance, Gaussian Model**

I. Introduction

Coconut (*Cocos nucifera*) has been grown in tropical regions for many years. This which belongs to the palm tree family is considered to be a multipurpose tree. The coconut is used for its water, oil, milk and flesh. Coconut oil is the tropical oil extracted from the flesh of the coconut. Many studies have proven, coconut oil to be one of the healthiest foods. The unique combination of fatty acids in coconut oil has positive effects on health, such as boosting fat loss, heart health, and brain function. Coconut oils are available in two varieties, virgin and refined oil. Virgin coconut oil is produced by cold pressing the liquid out of the meat while refined coconut oil is refined and processed through heat exposure.

However, it has been discovered that coconut oil is often adulterated with other edible oils and used coconut oil by suppliers. This compromises the safety of coconut oil making food prepared by using them unsafe for consumption. Mixing with used coconut oil makes it carcinogenic, increase LDL cholesterol causing obesity, weight gain and heart diseases.

In this paper it is focused on identification of adulteration of coconut oil using reused/reheated coconut oil. For this purpose, a multispectral imaging-based approach is utilized. A PCA based Bhattacharyya distance model is constructed to identify the adulteration level.

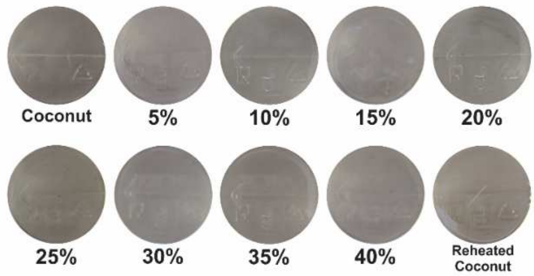

Fig. 1. RGB images captured from different adulteration levels.

II. Sample Preparation

For this research, freshly extracted coconut oil was obtained from Silver Mills Group, Mirigama, Sri Lanka, one of the renowned coconut oil producers and exporters in the country. For the analysis, pure coconut oil was adulterated with different concentrations of used coconut oil.

For the preparation of reheated oil samples, the process of deep-frying carefully prepared potato slices was followed. Potatoes obtained from the local market were washed thoroughly to remove soil, then, peeled off and sliced into pieces having approximately 4.5 cm diameter and 0.5 cm thickness. Prepared slices were blanched at 80 °C for 1 minute, blotted with a paper towel and packed in a sealed polythene bag before storing at -18 °C until further use. The experiment was carried out for 5 consecutive days using an oil sample of 1 liters. For each day, a batch from the processed potato chips was defrosted and the drip was blotted out ahead of the experiment. The oil sample was heated to 170 °C and the temperature was kept steady for 10 minutes. Then, 100g of the defrosted potato slices were fried for 3 minutes at a constant temperature range of 140-150 °C. Next, fried potato slices were removed from the oil sample. After letting the oil sample attain ambient temperature, multispectral images of the used oil sample were captured through the multispectral imaging [1] device. The same procedure was repeated for the oil sample for 5 consecutive days. As our main objective was to analyze the adulteration of reused/reheated coconut oil with pure coconut oil, finally, samples with different adulteration levels were created by mixing portions of reused oil samples into pure oil samples. Fig.1. shows RGB images of different adulteration levels.

III. MULTISPECTRAL IMAGING SYSTEM

In contrast with traditional RGB cameras, multispectral cameras provide rich information as they contain more spectral bands. However, multispectral cameras available in the market with high spectral and spatial resolutions are quite expensive. As implementing such expensive multispectral imaging systems for the use of small-scale industry is not viable, for this research an economical multispectral imaging system [2] was used. Fig.3. illustrates a schematic diagram of the imaging device. The mentioned multispectral imaging system has been successfully utilized in fish quality assessment [1], detection of adulterants in turmeric powder [3], assessment of meat quality [4], and Identification of Algae Contamination in High Voltage Insulators [5].

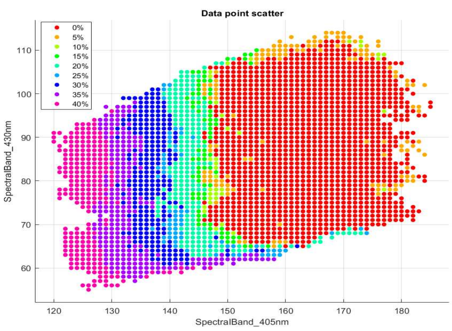

Fig. 2. Datapoint scatter between spectral band 405nm and Spectral band 430nm

TABLE I. LEDS OF THE MULTISPECTRAL IMAGING SYSTEM

LED No.	Details of the LEDs (UV, NIR and Visible)	Manufacturer Part Code	Bandwidth (nm)	Dominant Wavelength (nm)
1	*UV*	*VLMU3100*	*10*	*405*
2	*Visible*	*SM0603BWC*	*50*	*430*
3		*SM1204PGC*	*20*	*505*
4		*5973209202F-ND*	*10*	*590*
5		*5975112402F*	*20*	*660*
6	*NIR*	*QBHP684-IR4BU*	*20*	*740*
7		*VSMY2850G*	*10*	*850*
8		*VSMF4710-GS08*	*10*	*890*
9		*VSMS3700-GS08*	*20*	*950*

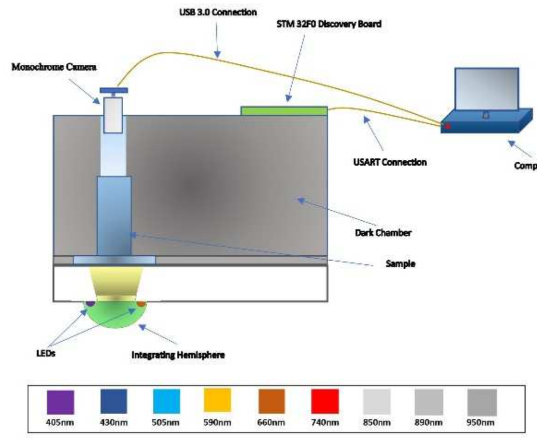

Fig.3. Inhouse build MSI system and its components

The imaging system used in this study consists of several major components as per Fig.3. A 10-bit CMOS monochrome camera (FLIR Blackfly S Mono,1.3 MP, USB3 Vision camera, Resolution – 1280×1024) was mounted on top of the portable dark chamber to capture the transmittance spectrum of a sample. The portable lighting chamber comprises nine narrow band LEDs with wavelengths ranging from 405 nm to 950 nm as shown in the Table 1. This imaging system has the capability of capturing monochrome multispectral images from Ultra-Violet(UV) to Near Infra-Red (NIR) having a resolution of nine spectral bands.

IV. PREPROCESSING

Captured monochrome images are subjected to different types of noise such as quantization noise, amplifier noise, non-uniform illumination, sensitivity variation of detectors and dust. Due to this fact, it is essential to perform several image processing techniques to reduce the noise effect. Initially, the dark current reduction is carried out [6]. The dark current image captured at the close shutter state is subtracted from each multispectral image as per the following equation.

$$\mathrm{B}[\lambda] = \mathrm{A}[\lambda] - D \quad (1)$$

where $\mathrm{B}[\lambda]$ is the dark current removed image at wavelength λ, $\mathrm{A}[\lambda]$ is the original image at wavelength λ and D is the dark current image.

Next, to remove the random noise nonlinear median filtering [7] is applied on the dark current subtracted image.

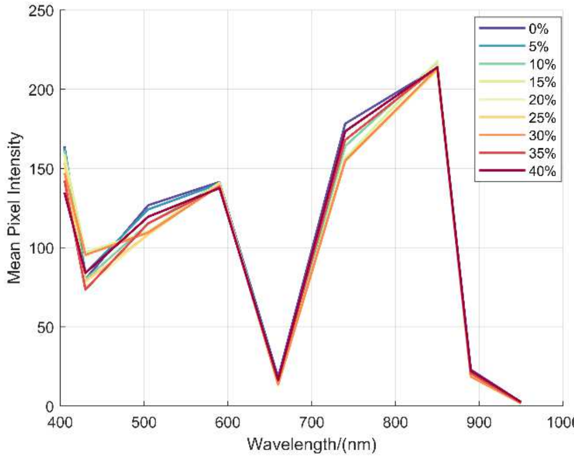

Fig.4. Spectral signature for different adulteration levels.

V. Spectral Signature

To seek the viability of identifying different adulteration levels, the spectral signatures of images corresponding to each adulteration level were compared. The spectral signatures of the samples were computed using the preprocessed images, following the procedure mentioned below.

A. Procedure

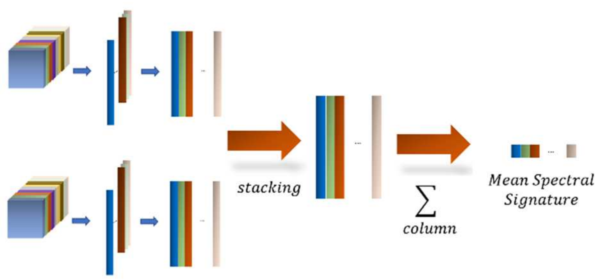

Fig.5. Procedure to obtain the spectral signatures

Initially, a 30x30 pixel window from the multispectral image was selected by manual inspection. Then, keeping the coordinates and the size constant the pixel windows were extracted from images corresponding to all the adulteration levels.

For this, 15 images from each adulteration level were considered. Then, the data matrix for a single adulteration level was prepared, by stacking pixel values of each pixel window corresponding to each spectral band reshaped as column vectors. The final dimension of the matrix was 13500*9. Thereafter, the mean spectral signature was obtained by computing the mean of 13500 rows as shown Fig.5. The same procedure was followed for every adulteration level. The Fig.4. indicates the mean spectral signature for each adulteration level.

As can be seen from Fig. 4, there is a noticeable difference in the 450nm-500nm and 750nm-800nm ranges. Therefore, the obtained multispectral images can be used in identifying different adulteration levels.

VI. Analysis

A. Dimension Reduction through PCA

Principal Component Analysis [8] is a widely used linear transformation tool that can be used for dimension reduction, data compression and data visualization. The key idea of PCA is to reduce the dimensionality of a data set consisting of a large number of interrelated variables, while retaining most of the variation present in the data set. This is achieved by transforming to a new set of variables, the principal components (PCs), which are uncorrelated, and which are ordered so that the first few retain most of the variation present in all of the original variables.

The data set,

$$[X_1 \quad X_2 \quad X_3 \quad \ldots \quad X_9]$$

Where, X_i contains stacked datapoints corresponding to i^{th} spectral band.

Step 1: Calculating the mean vector ($\hat{m}$) and variance ($\hat{\sigma}^2$) of the dataset.

$$\hat{m} = \frac{1}{N}\sum_{k=1}^{N} x_k \qquad (2)$$

$$(\hat{\sigma}^2) = \frac{1}{N}\sum_{k=1}^{N}(x_k - \hat{m})^2 \qquad (3)$$

Where: x_k = k th data point
N = Total number of data points
$\hat{\sigma}$ = Standard Deviation

Step 2: Standardization.

This step aims to standardize the range of the initial variables so that each of them contributes equally to the analysis.

$$z_k = \frac{x_k - \hat{m}}{\hat{\sigma}} \qquad (4)$$

Where: z_k = standardized k^{th} datapoint

Step 3: Calculating the covariance matrix (C).

To extract the correlation among the spectral bands.

$$C = \frac{1}{N}\sum_{k=1}^{N}(x_k - \hat{m})(x_k - \hat{m})^T \qquad (5)$$

Step 4: Calculating eigenvalues (λ_n) and eigenvectors (v_n) of C.

Find the roots of the characteristic equation to determine the eigenvalues.

$$|C - \lambda I| = 0 \qquad (6)$$

Step 5: Projection on to Principal Components.

$$y = [v_1 \ v_2 \ v_3 \ldots . \ v_n]^T x \qquad (7)$$

Where: $\qquad$ y = Transformed data set

v_p = p^{th} eigenvector of C

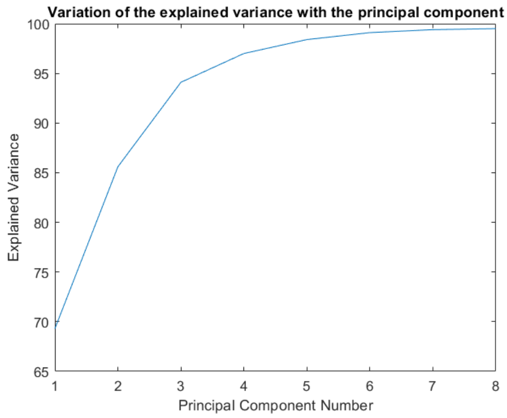

Fig. 6. Variation of explained variance with the principal component number

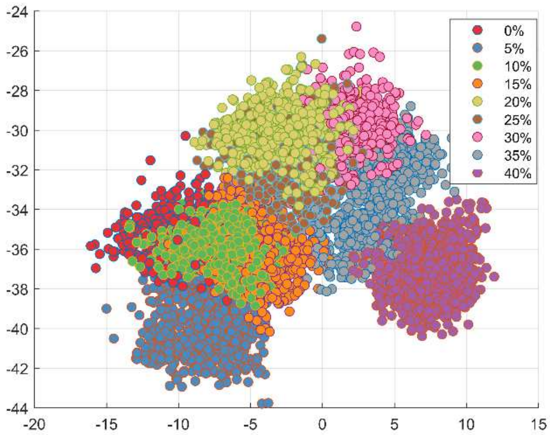

Fig .7. Projected oil dataset onto first two PCs

Fig.6. shows the variation of explained variance with the number of eigenvalues. From Fig.6. it was evident that the highest five eigenvalues were sufficient to explain the dataset up to 99%. Fig.7. illustrates the projected data point onto first two eigen vectors.

B. Model Construction through Bhattachrayya Distance

To establish a functional relationship among the adulteration levels Bhattacharya distance [5],[9],[10] was utilized. Bhattacharya distance measures the correlation of two normally distributed probability density functions as per equation (8).

In this research above metric was used to measure the separability among the adulteration levels. The directions given by eigenvectors of the data covariance matrix were used to observe spectral density values of each adulteration level. The obtained pixel intensity histograms for each eigen direction followed a Gaussian distribution. Fig.8. shows the projected pixel intensity histogram to the highest variance direction of the covariance matrix. As 99% of dataset can be explained through dominant five principal components, the probability distribution of each adulteration was approximated by a five-dimensional multivariate Gaussian distribution.

$$B(S_{ref}, S_{ds}) = (\mu_{ref} - \mu_{ds})^T \left(\frac{C_{ref} - C_{ds}}{2}\right)^{-1} (\mu_{ref} - \mu_{ds}) + \frac{1}{2} ln \left(\frac{\left(\frac{C_{ref} - C_{ds}}{2}\right)}{\sqrt{|C_{ref}||C_{ds}|}} \right) \qquad (8)$$

where, $B(S_{ref}, S_{ds})$is the Bhattacharyya distance between two multivariate Gaussian distribution functions S_{ref} and S_{ds}; μ_{ref}, μ_{ds} are the mean vectors; and C_{ref}, C_{ds} are the covariance matrices of classes S_{ref} and S_{ds} respectively.

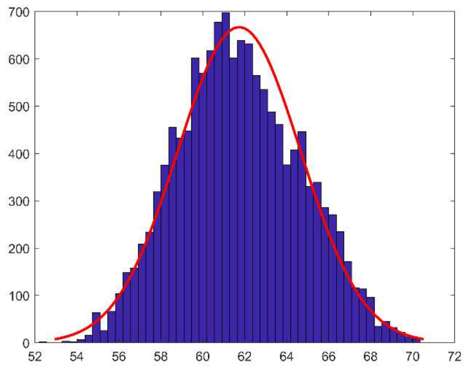

Fig.8. Projected pixel intensity histogram to the highest variance direction of the covariance matrix.

VII. Result and Discussion

A functional relationship was established between the Bhattacharyya distance and adulteration level as shown in Fig.9. The above metric was calculated for all 15 replicated from each adulteration level. A randomly selected 900 data points from the class were used as the reference in calculating the metric. For the generation of the functional relationship, the mean of 15 replicates was selected. The generated functional relationship for normalized Bhattacharyya is,

$$Y = 3.93X^2 + 0.258X + 0.1 \qquad (9)$$

with $R^2 = 0.9747$.

Where X, Y represent the percentage adulteration level and the Bhattacharyya distance respectively.

From the relationship observed, it can be stated that the Bhattacharyya distance increases with the adulteration level. Construction of the multivariate Gaussian model and the derivation of a functional relationship between the Bhattacharyya distance and the adulteration levels permits computing an unknown adulteration level of a coconut oil sample. Hence, this model can be successfully utilized in identifying the adulteration using reused/reheated coconut oil through multispectral imaging.

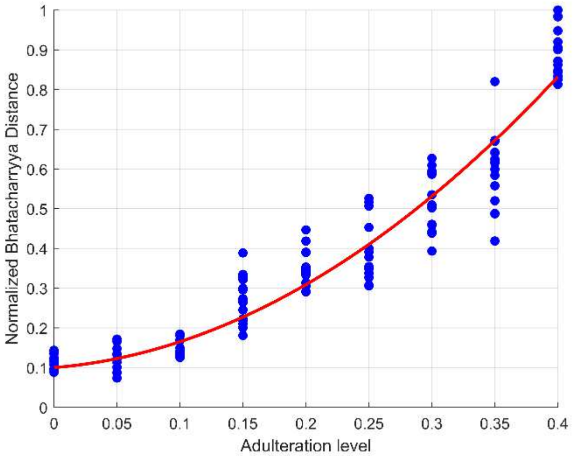

Fig. 9. Variation of mean Bhattacharyya distance with reheated coconut oil adulteration level

REFERENCES

[1] Jayasundara, Dhananjaya & Ramanayake, Lakshitha & Senarath, Neranjan & Herath, Sanjaya & Godaliyadda, G M Roshan & Ekanayake, Mervyn Parakrama & Herath, Vijitha & Ariyawansa, Sujeewa. (2020). Multispectral Imaging for Automated Fish Quality Grading. 321-326. 10.1109/ICIIS51140.2020.9342726.

[2] Odoom, & Bart-Plange, A. & Darko, & Addo, Ahmad. (2014). Quality assessment of moisture content, free fatty acids and acid value of coconut oil produced in the Jomoro District of the Western Region of Ghana. Journal of Research in Agriculture: An International Scientific Research Journal. 3. 205-210.

[3] Nasrullah, Nasrullah. (2020). Quality assessment and safety measurement of different industrial processing stages of soybean oil. Turkish Journal of Food and Agriculture Sciences. 10.14744/turkjfas.2019.006.

[4] Ramanayake, R.M.L.S & Senarath, H.M.N.B & Jayasundara J.V.M.D.B & Prabath, G.W.K & Weerasooriya, H.M.H.K & Fernando, M.A.R.M & Kumara, S & Herath, H.M.V.R & Godaliyadda, G.M.R.I & Ekanayake, M.P.B & Athukorala, S. (2021). Reflectance Multispectral Imaging for Identification of Algae Contamination in High Voltage Insulators. (unpublished)

[5] Sivaramakrishnan, Anand & Morse, Ernie & Makidon, Russell & Bergeron, Louis & Casertano, Stefano & Figer, Donald & Acton, Daniel & Atcheson, Paul & Rieke, Marcia. (2004). Limits on routine wavefront sensing with NIRCam on JWST. Proc SPIE. 10.1117/12.551243

[6] Ivković, Ratko & Milošević, Ivana & Petrović, Mile & Gvozdic, Branko. (2015). Timeline of Median filter. 268-273. 10.15308/Synthesis-2015-268-273.

[7] Mishra, Sidharth & Sarkar, Uttam & Taraphder, Subhash & Datta, Sanjoy & Swain, Devi & Saikhom, Reshma & Panda, Sasmita & Laishram, Menalsh. (2017). Principal Component Analysis. International Journal of Livestock Research. 1. 10.5455/ijlr.20170415115235.

[8] Choi, Euisun & Lee, Chulhee. (2003). Feature extraction based on the Bhattacharyya distance. Pattern Recognition. 36. 1703-1709. 10.1016/S0031-3203(03)00035-9

[9] Weerasooriya, Kavinga & Herath, Sanjaya & Ranasinghe, Don Yasiru & Bandara, Chaminda & Herath, Vijitha & Godaliyadda, G M Roshan & Ekanayake, Mervyn Parakrama & Madhujith, Terrence. (2020). Transmittance Multispectral Imaging for Edible Oil Quality Assessment